MARY KAY O'CONNOR PROCESS SAFETY CENTER
TEXAS A&M ENGINEERING EXPERIMENT STATION

19th Annual International Symposium
October 25-27, 2016 • College Station, Texas

Thermal Decomposition Mechanisms of 1H-1,2,4-Triazole Derivatives : Theoretical Study

Wasana Kowhakul *, Daisuke Inoue, Yuki Nakagawa, Hiroshi Masamoto, Mikiji Shigematsu

Department of Chemical Engineering, Faculty of Engineering, Fukuoka University, Fukuoka 814-0180, JAPAN

†Presenter E-mail: kowhakulw@fukuoka-u.ac.jp

Abstract

In the present work, T_{DSC} of 1Htri, 1Htri-CH_3 and 1Htri-NH_2 were determined by using SC-DSC and Molecular orbital calculations (MO) was used to clarify thermal decomposition mechanism and stability criteria of pathway of 1Htri, 1Htri-CH_3 and 1Htri-NH_2 were d.

T_{DSC} of 1Htri, 1Htri-CH_3 and 1Htri-NH_2 were determined from the lower ΔEa of thermal decomposition pathway model as proton transfer combine with cleavage bond. The determined T_{DSC} were 297 ºC of 1Htri, 114 ºC of 1Hti-CH_3 and 289 ºC of 1Htri-NH_2.There results were corresponded with the measured T_{DSC} as were 338 ºC of 1Htri, 172 ºC of 1Hti-CH_3 and 293 ºC of 1Htri-NH_2, respectively.

The results reveal that our approach thermal decomposition pathway model as combination of proton transfer and cleavage bonds of 1Htri, 1Htri-CH_3 and 1Htri-NH_2 cab be possible to expand and control the application of these compounds.

Keywords: *1H-1,2,4-triazole, 3-amino-1,2,4-triazole, 3-methyl-1H-1,2,4-triazole, thermal decomposition, molecular orbital calculation*

1. Introduction

Triazoles and their derivatives have the high nitrogen content and density, good thermal stability, low impact sensitivity and high explosive volume, low molecular weight, and because of these they can be used both for civil and military application such as explosives, propellants and pyrotechnics. Several groups have focused on theoretical and experimental studies to understand the thermal decomposition mechanism and stability criteria of different types of 1,2,4-triazols.

However, the characteristic energy generation has not understand clearly. If these effects were understood, it would be possible to expand and control the application of these energy-providing materials [1-6].

Rao et al. examined the thermal decomposition and energetic 1,2,4-triazole derivatives using a photoacoustic (PA) and TG-DTA techniques, the study investigated during 30-350ºC rang , the thermal energy is released in multiple step and high density of compounds leads to higher strength of photoacoustic. The released quantity of gaseous products was measured interms of the strength of PA signal which depends on the density of compounds. However, thermal decomposition mechanism and stability criteria are not approach [7].

In the present study, the influence of the ($-CH_3$) and ($-NH_2$) substituents on the thermal decomposition (T_{DSC}) of 1H-1,2,4-triazole (1Htri) were determined by using SC-DSC. Molecular orbital calculations (MO) were used to clarify thermal decomposition mechanism and stability criteria of pathway of 1Htri, 3-methyl-1H-1,2,4-triazole (1Htri-CH_3) and 3-amino-1H,2,4 -triazole (1Htri-NH_2) were calculated. T_{DSC} of each compound was determined from lower ΔEa of thermal decomposition pathway model selection. The determined T_{DSC} of 1Htri, 1Htri-CH_3 and 1Htri-NH_2 were compared with the measured T_{DSC}.

Molecular structure of 1Htri, 1Htri-CH_3 and 1Htri-NH_2 were shown in fig.1.

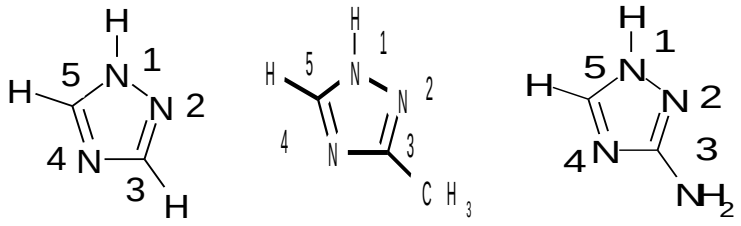

(i) (ii) (iii)

Fig. 1. Molecular structure of (i) 1H-1,2,4-triazole, (ii) 3-methyl-1H-1,2,4-triazole (iii) 3-amino-1H,2,4-triazole

The layout of the paper is as follow. In section 2 the experimental set-up and the experiment procedure are described. In section 3 the experimental results and analytical predictions are given. Section 4 include the conclusions.

2. Experiment

2.1 Materials

2.1 Materials

1Htri, 1Htri-NH_2 (all 98.0%, Tokyo Chemical Industry) and 1Htri-CH_3 (95%, Wako Pure Chemical Industries, Japan) were used in the test work.

2.2 Thermal analysis

To investigate the thermal decomposition, SC-DSC (6220 SII nanotechnology) was carried out in a stainless steel cell at a heating rate of 10 K min-1 from 30 to 500°C under a steady state flow of air using a 1.0 mg sample.

2.3 Molecular orbital calculations

To obtain an understanding of the thermal and chemical properties of 1Htri when coordinated with a substituent as CH_3 and NH_2, MO were conducted using the Spartan'10. Geometric optimization of the structures and vibration analyses were achieved using unrestricted B3LYP/6-31+G* density functional theory (DFT). The influence of substituent on (1) bond distance, (2) ΔEa and G-G^0 (ΔG)

First, the molecular structure was built on the screen, and the optimal structure at ground state was obtained. Next, to obtain the transition state of cleavage of 5 members ring, the energy change depend on the distances of two single bonds which were specified from 3 single bonds was calculated. Saddle point was found out from the energy map and optimized the transition state (TS). Then, the ΔEa and ΔG was obtained as the difference of the energies between TS and ground state (GS).

3. Results and Discussions

3.1. Search of transition state of 1Htri, 1Htri-CH3 and 1Htri-NH_2 derivatives

Table 1 shows the bond distance in ring of 1Htri, 1Htri-CH_3 and 1Htri-NH_2. From these values, it can be considered that even though 1Htri coordinated with derivatives, the longer distance bonds position as N1-N2, C3-N4 and C5-N1 are not change.

Table 1. Bond distance and the bond order in ring of 1Htri,1Htri-CH_3 and 1Htri-NH_2 at ground state

Bond	Distance [Å]		
	1Htri	1Htri-NH_2	1Htri-CH_3
N1-N2	1.357	1.369	1.358
N2=C3	1.326	1.331	1.330
C3-N4	1.365	1.369	1.371
N4=C5	1.323	1.323	1.322
C5-N1	1.352	1.346	1.350

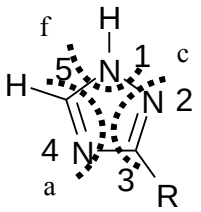

R= H, CH_3, NH_2

Fig.2 Combinations of three ways are (a) N1-N2 and C5-N1, (c) N1-N2 and N3-N4, (f) N3-N4 and C5-N1of initial decomposition should start.

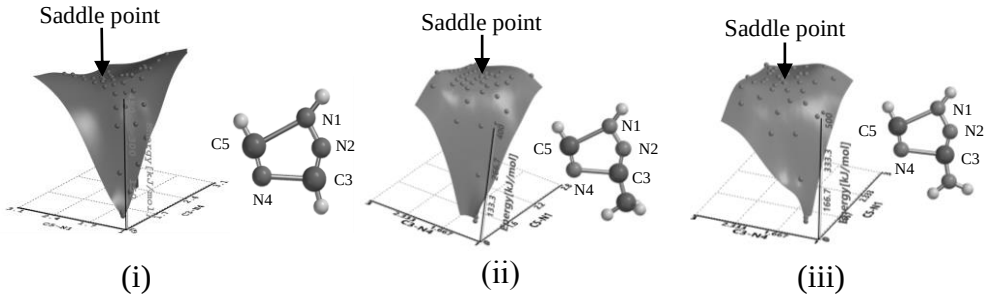

Fig.3 Energy map at TS of (a) C5-N1 and C3-N4 cleavage of 1Htri, 1Htri-CH_3 and 1Htri-NH_2

Table 2 ΔEa , $\Delta G_{25°C}$ and ΔG_{Tdsc} at TS of1Htri, 1Htri-NH_2 and 1Htri-CH_3

Substance	Cleavage bonds	ΔEa [kJ/mol]	$\Delta G_{25°C}$ [kJ/mol]	ΔG_{Tdsc} [kJ/mol]
1Htri	a	379	350	338
	c	439	398	378
	f	over 540		
1Htri-NH_2	a	419	390	387
	c	434	403	398
	f	over 650		
1Htri-CH_3	a	365	416	405
	c	420	381	373
	f	over 600		

Fig.2 and Fig. 3 show the combination initial decomposition should start and each energy map of 1Htri, 1Htri-CH_3 and 1Htri-NH_2 at TS.

For example, the cleavage by the combination in case of (c) N1-N2 and C3-N4. The energy increased with increase of two distances of N1-N2 and C3-N4, however, decreased with excessive distances. The saddle point appeared around 2.323 Å of N1-C5 and 2.090 Å of C3-N4 in case of 1Htri, around 2.221 Å of N1-C5 and 2.169 Å of C3-N4 in case of 1Htri-NH_2 and around 2.220 Å of N1-C5 and 2.178 Å of C3-N4 in case of 1Htri-CH_3.

From this saddle point, the TS was determined by further optimization. Table 2 shows the bond distance at TS of each cleavage (a), (c) and (f) of 1Htri, 1Htri-CH_3 and 1Htri-NH_2, respectively.

3.2 Activation energy determination of 1Htri, 1Htri-CH_3 and 1Htri-NH_2 under no translation of proton condition

Table 3 shows the ΔEa of three ways decompositions of all 1Htri, 1Htri-CH_3 and 1Htri-NH_2 were calculated under limited condition as no translation of proton.

Fig. 4-6 shows the ΔEa at TS of each (a) C3-N4 and C5-N1 and (c) N1-N2 and C3-N4 cleavage of 1Htri, 1Htri-CH_3 and 1Htri-NH_2.

Due to ΔEa, it can be consider that the combination of cleavage bonds were maintained to the combination of (a) C3-N4 and C5-N4 cleavage of 1Htri, 1Htri-CH_3 and 1Htri-NH_2.

Table 3. Structure of 1Htri at the initial step of the thermal decomposition

Cleavage bonds	Distance [Å]					ΔEa [kJ/mol]	$\Delta G_{25°C}$ [kJ/mol]	$\Delta G_{T_{dsc}=338°C}$ [kJ/mol]
	N1-N2	N2-C3	C3-N4	N4-C5	C5-N1			
Ba	1.281	1.203	2.090	1.174	2.323	379	350	338
Bc	2.852	1.175	1.985	1.277	1.274	439	398	378
A1Be	1.281	2.323	1.174	2.090	1.203	379	350	338
A1Bd	2.852	1.274	1.277	1.985	1.175	439	398	378
A2Bc	Not optimized							
A1A)C5→N4d	Not optimized							
A2Bd	Not optimized							
A1A)C5→N4c	Not optimized							
A2Be	Not optimized							
A1A)C5→N4a	Not optimized							
A3Ba	Not optimized					over500		
A1A)C5→N1e	Not optimized					over600		
A3Bb	Not optimized							
A1A)C5→N1b	Not optimized							
A3Bc	Not optimized							
A1A)C5→N1d	Not optimized							
A4Ba	1.264	1.190	2.537	1.219	2.089	475	440	430
A1A)C3→N4e	1.264	2.089	1.219	2.537	1.190	475	440	430
A4Bc	2.301	1.205	1.750	1.282	1.226	289	263	253
A1A)C3→N4d	2.301	1.226	1.282	1.750	1.205	289	263	253
A4Bd	2.161	1.268	1.277	2.594	1.199	497	455	433
A1A)C3→N4c	2.161	1.199	2.594	1.277	1.268	497	455	433
A2A)N1→N2a	Not optimized							
A2A)N1→N2c	Not optimized							
A2A)N1→N2d	Not optimized							
A3A)C5→N4c A4A)C3→N2c	Not optimized							
A3A)C5→N4d A4A)C3→N2d	Not optimized							
A4A)N1→C5c	2.137	1.165	2.594	1.283	1.268	412	374	356
A4A)N1→C5d	2.138	1.268	1.283	2.596	1.164	412	374	356

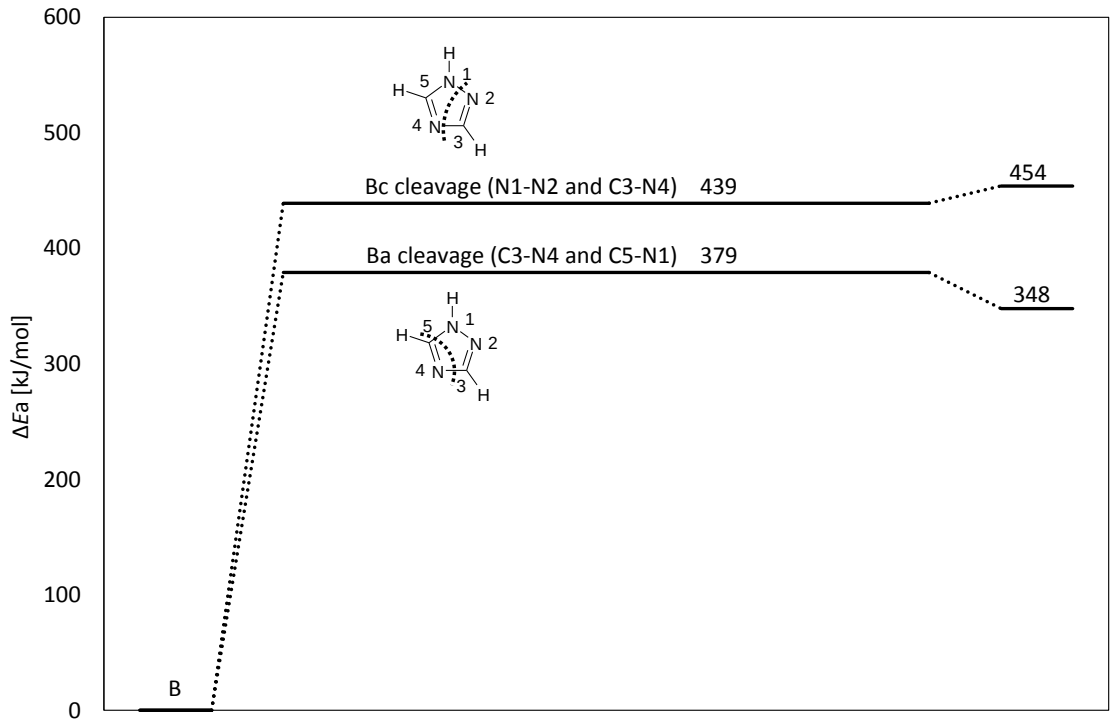

Fig.4 ΔEa map at (Ba) C5-N1 and C3-N4 cleavage and (Bc) N1-N2 and C3-N4 cleavage of 1Htri

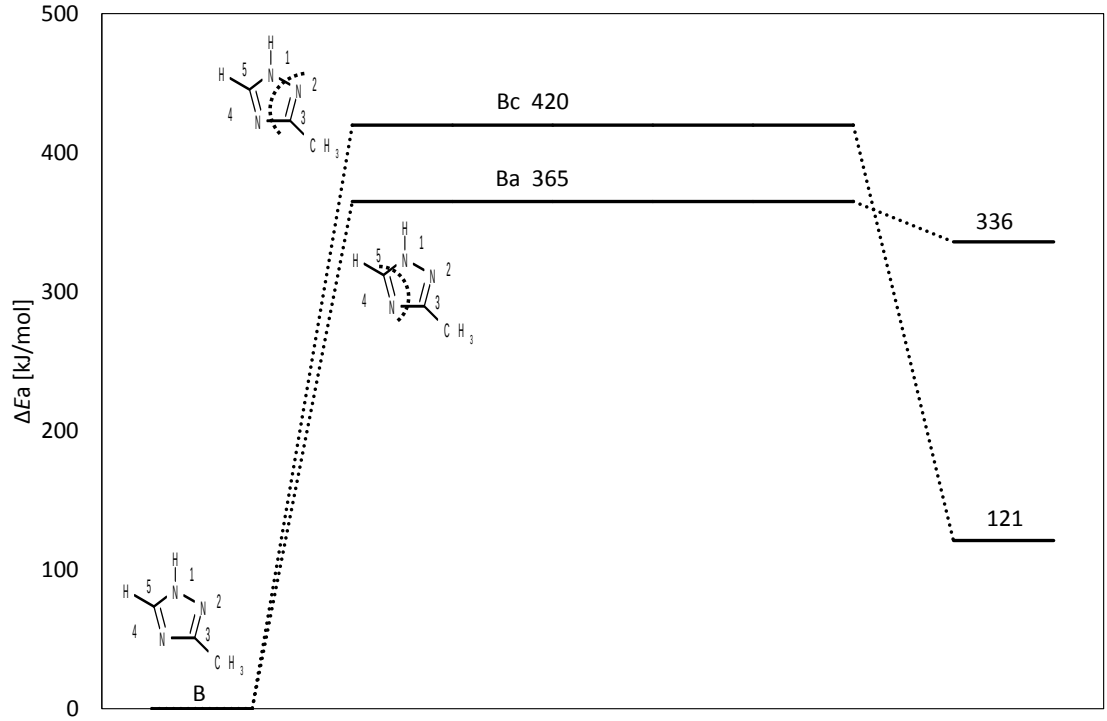

Fig.5 ΔEa map at (Ba) C5-N1 and C3-N4 cleavage and (Bc) N1-N2 and C3-N4 cleavage of 1Htri-CH_3

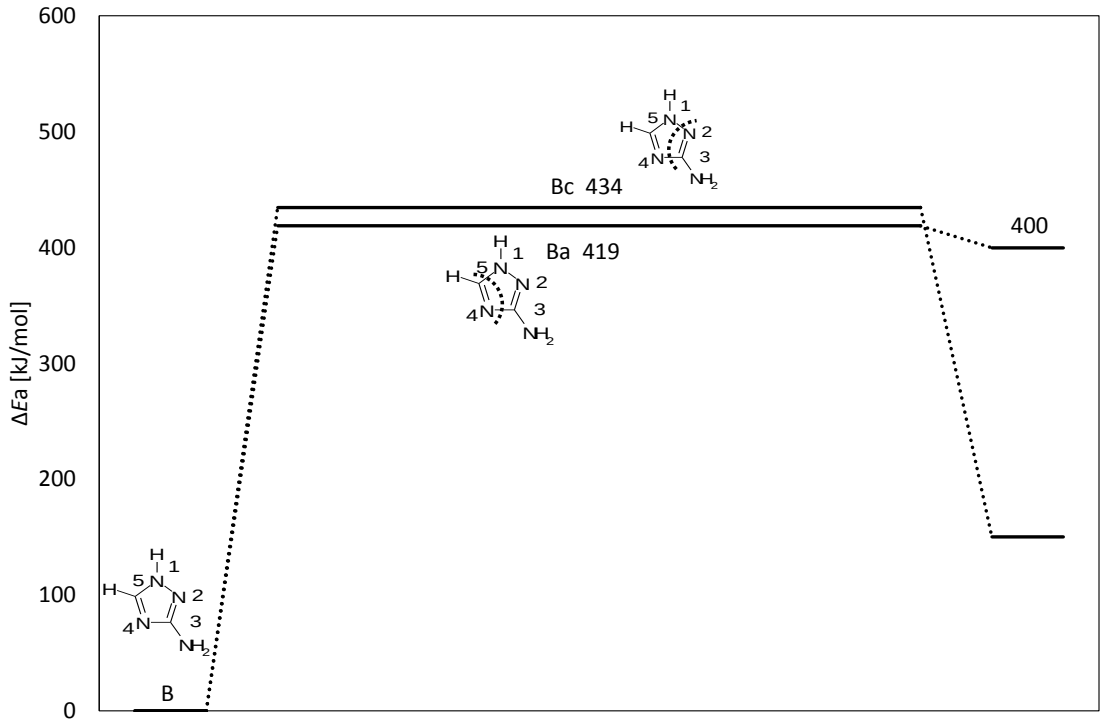

Fig.6 ΔEa map at (Ba) C5-N1 and C3-N4 cleavage and (Bc) N1-N2 and C3-N4 cleavage of 1Htri-NH_2

3.3 Activation energy Determination of 1Htri under translation of proton condition

As shows in section 3.2 the calculated under no proton translation pathway.

M.Tabatabee et al examined thermal behavior of 4Htri changed to 3Htri form then reaction occur (see fig.7). However, the present case, the mechanisms have not clarify. Therefore, in this study, thermal decomposition pathway of 1Htri, 1Htri-CH_3 and 1Htri-NH_2 were also considered under translation of proton condition.

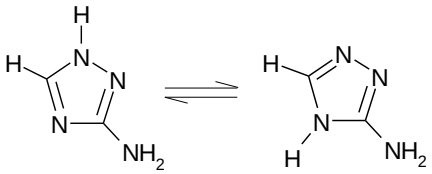

*E*a=-781369.98 [kJ/mol] *E*a=-781411.27 [kJ/mol]

3-amino-1H-1,2,4-triazole 3-amino-4H-1,2,4-triazole

Fig.7 1,3-sigmatropic hydrogen shift in 3-amino-1Htri and formation of 3-amino-4Htri

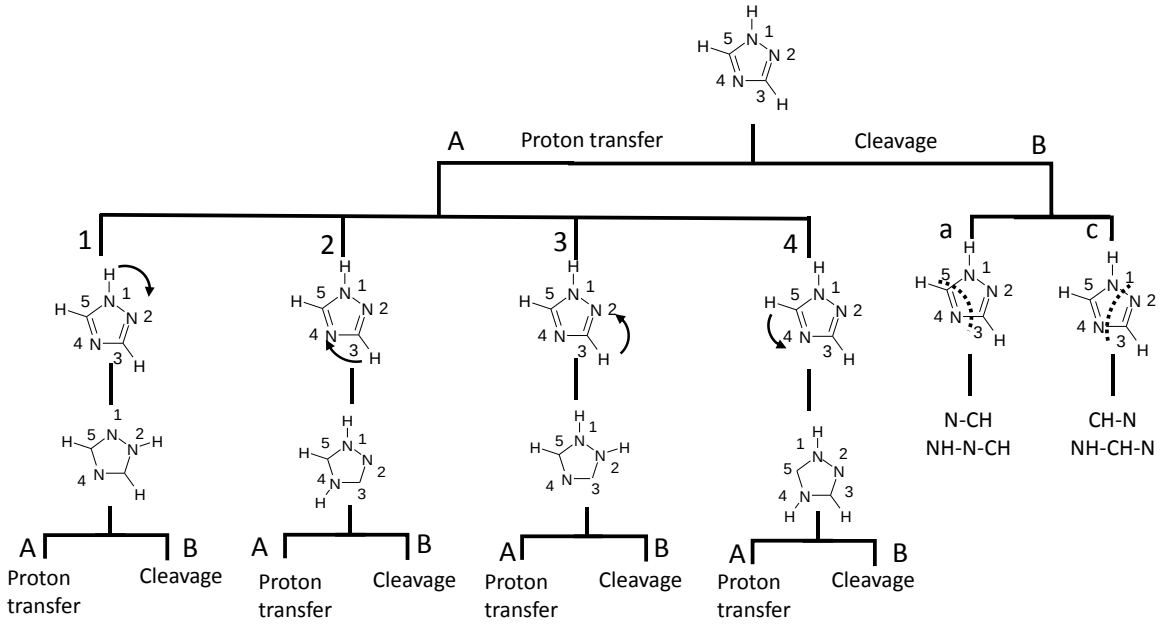

Fig.8 Thermal decomposition pathway at (A) proton transfer and (B) cleavage of 1Htri.

Fig. 8 shows there are two possible thermal decomposition pathways assumption of 1Htri as (A) proton transfer at first state and (B) bond cleavage at first state.

In case of (B) bond cleavage occur at the first state, the decomposition should start at two single bonds of the single bonds as section 3.2 we consider that there is a relationship between bond distance and decomposition and assume that long bonds tend to become disconnected.

ΔEa of cleavage bounds of each (a) N1-C5 and C3-N4, (c) N1-N2 and C3-N4, (f) N1-N2 and N1-C5 of 1Htri is shown in Table 2. With these ΔEa values, it can be considered that the combination of (a) N1-C5 and C3-N4 shows lower ΔEa comparing other (c) and (f) cleavage pattern then the decomposition of 1Htri will start preferentially at (a) N1-C5 and C3-N4.

As shows in fig.8, if proton transfer at first state, there are four possible combinations as (A1) proton transfer from N1→N2, (A2) proton transfer from C3→N4, (A3) proton transfer from C3 →N4 and (A4) proton transfer from C5→N4.

However, only A1 as shows in fig.9 and A4 as shows in fig.12 were possible to find the T.S. but cannot observe T.S. as A2 as shows in fig.10 and A3 as shows in fig.11.

Fig. 13 and fig.14 show energy flow chart of A1 and A4 with this energy chart, it can be considered that pathway A1A)C3→N4d.

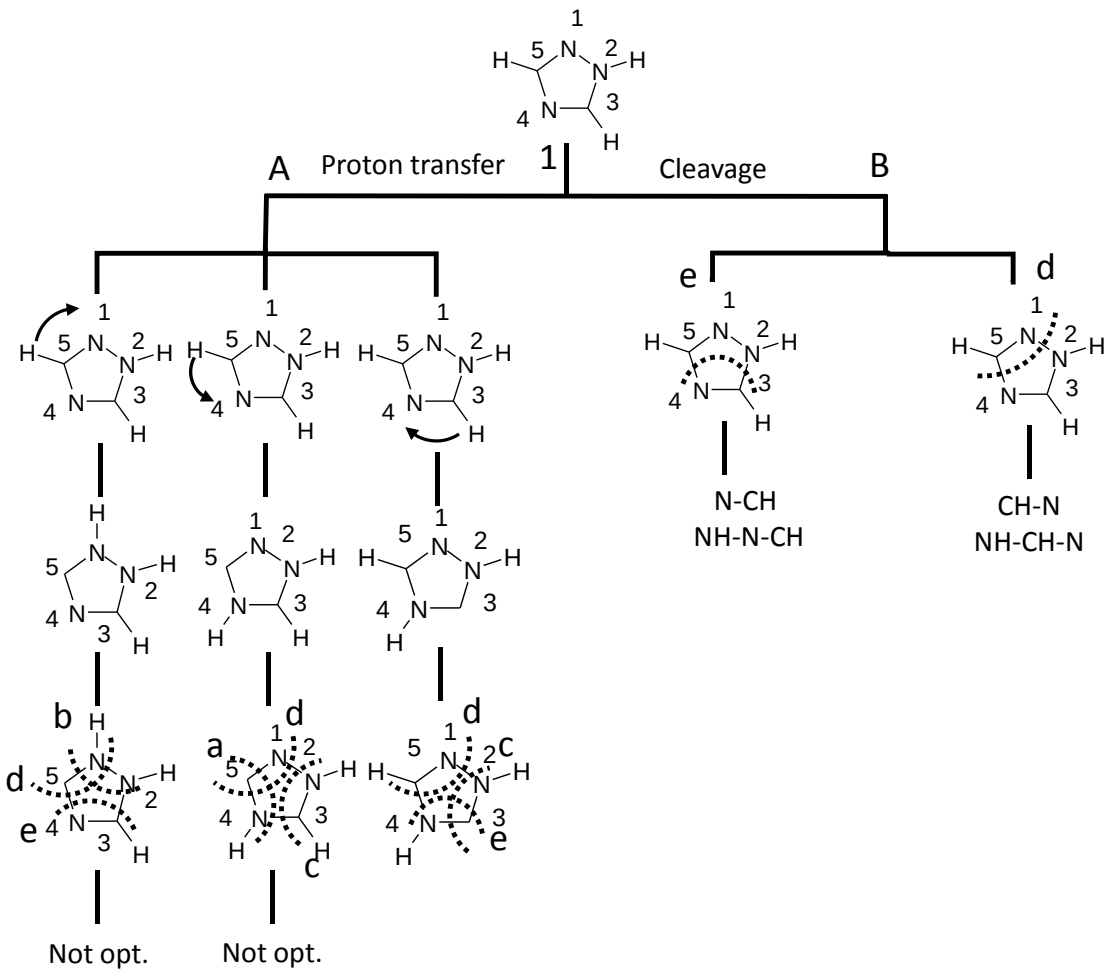

Fig.9 Thermal decomposition pathway at (A1A) proton transfer and (A1B) cleavage of 1Htri.

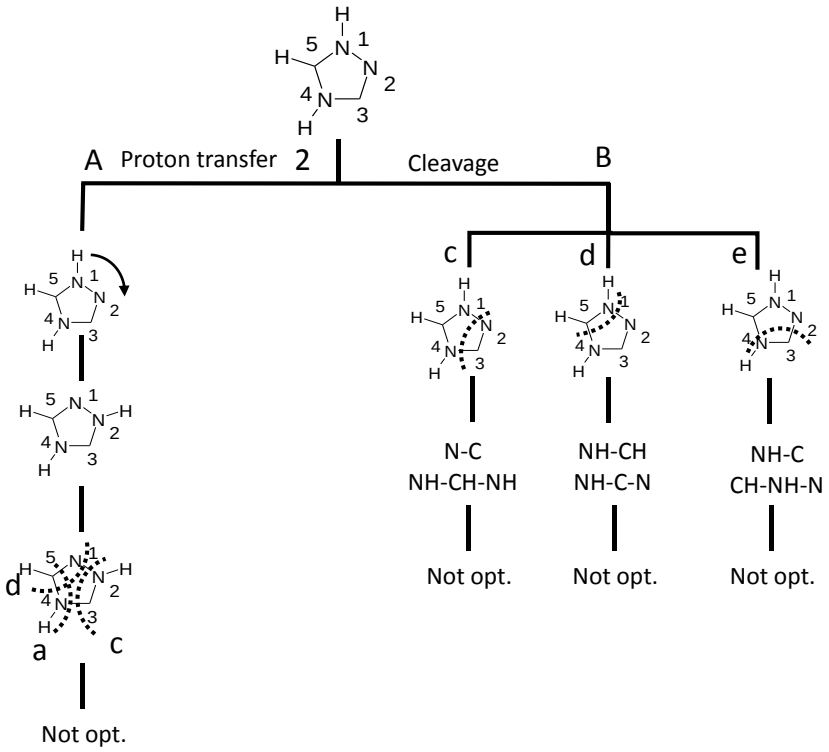

Fig.10 Thermal decomposition pathway at (A2A) proton transfer and (A2B) cleavage of 1Htri.

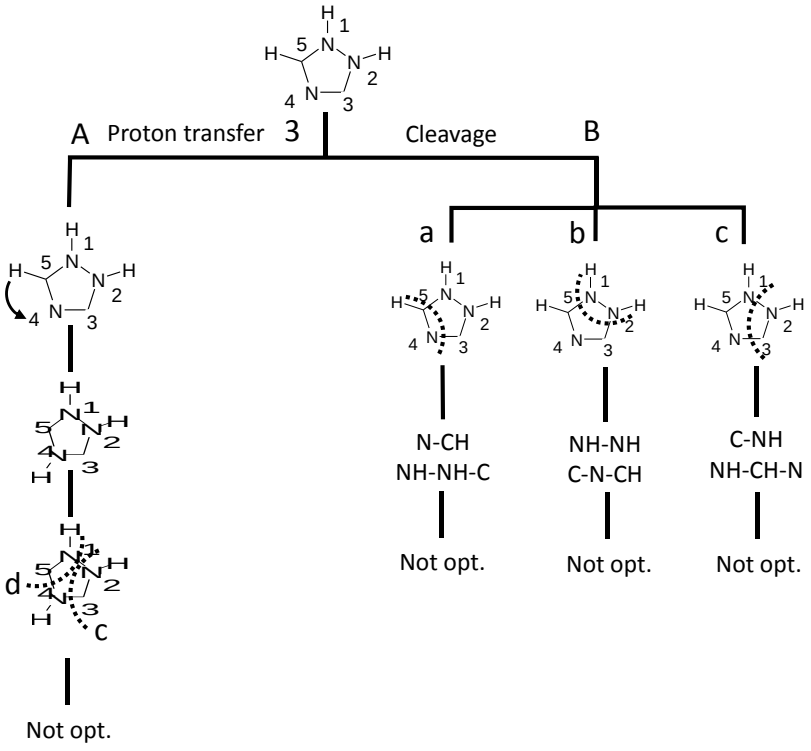

Fig.11 Thermal decomposition pathway at (A3A) proton transfer and (A3B) cleavage of 1Htri.

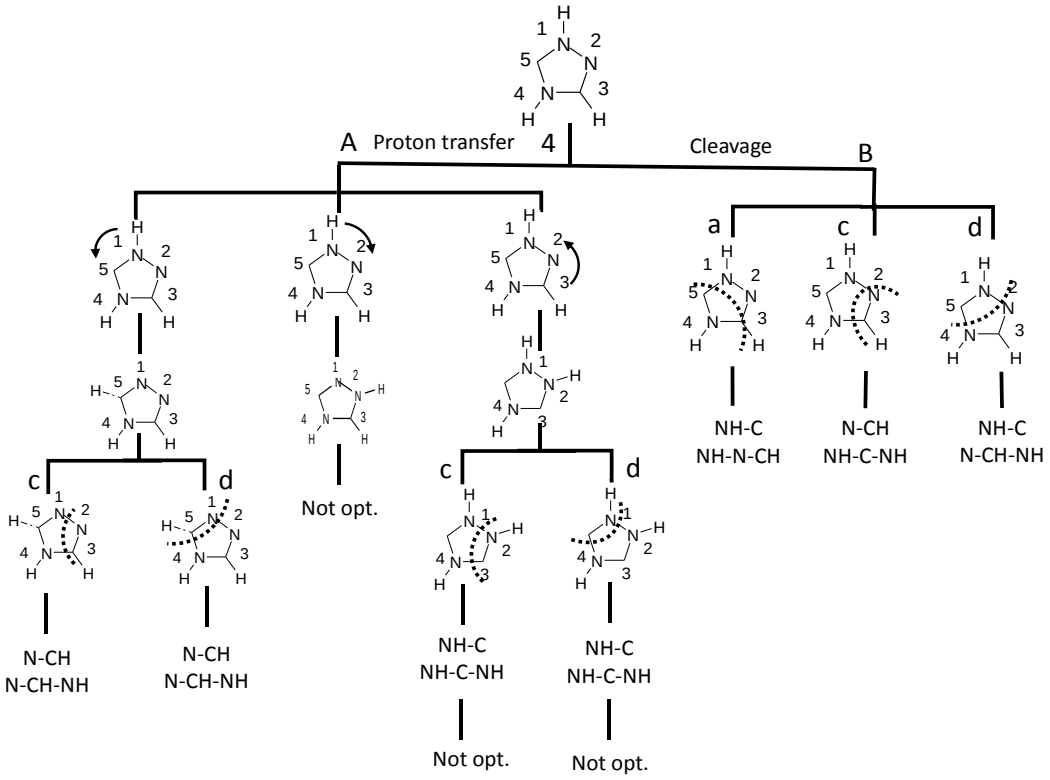

Fig.12 Thermal decomposition pathway map at (A4A) proton transfer and (A4B) cleavage of 1Htri.

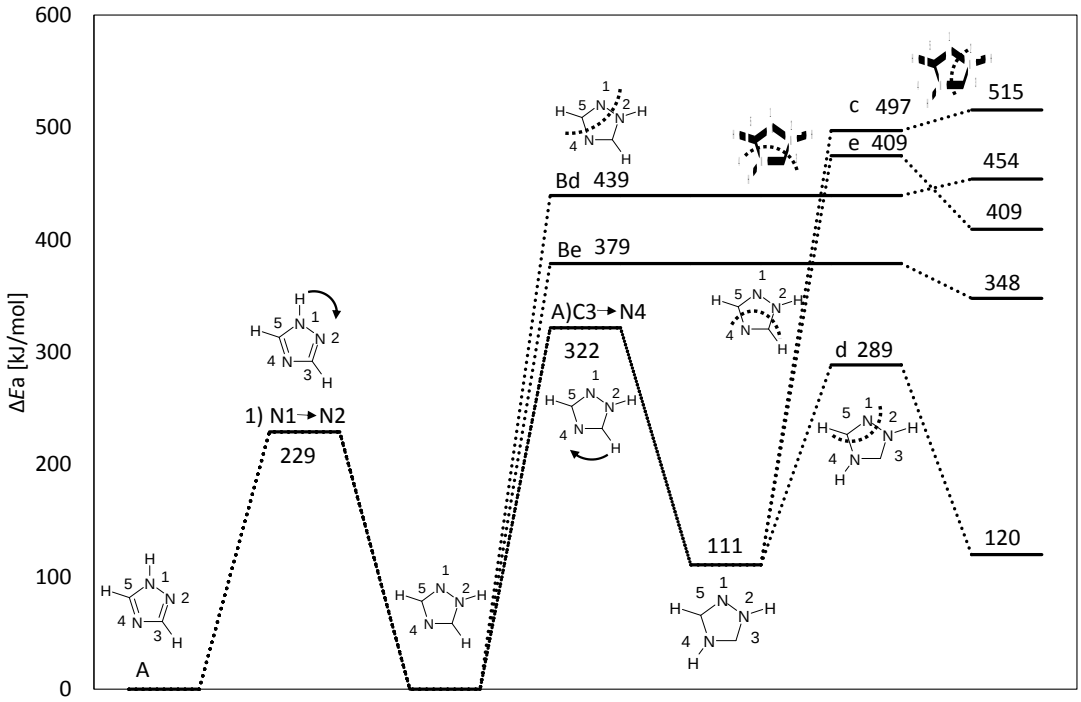

Fig. 13 Thermal decomposition pathway map at A1A)C3→ N4c,d,e, A1Be and A1Bd of 1Htri.

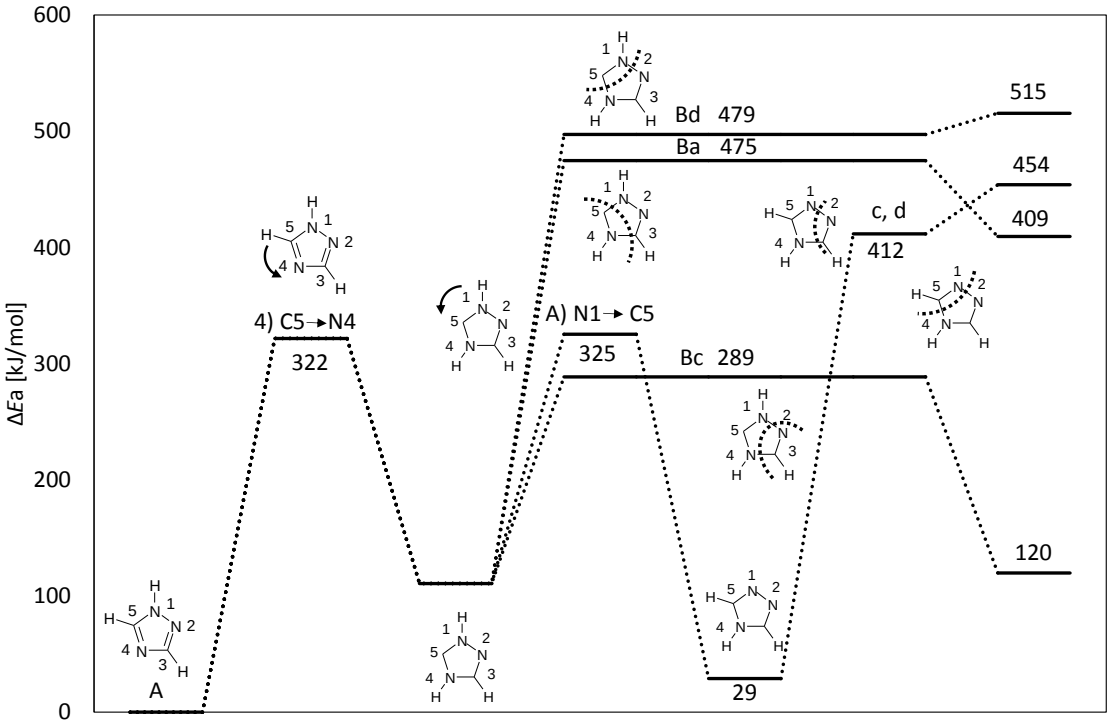

Fig. 14 Thermal decomposition pathway map at A4A)N1→ C5c,d, A4Ba,c,d

Table 4 The produced gases after each decomposition pathway of 1Htri

Cleavage bonds	Gas
Ba, A1Be	N-CH, NH-N-CH
Bc, A1Bd, A4A)N1→C5c, A4A)N1→C5d	CH-N, NH-CH-N
A2Bc, A1A)C5→N4d	N-C, NH-CH-NH
A2Bd, A1A)C5→N4c	NH-CH, NH-C-N
A2Be, A1A)C5→N4a	NH-C, CH-NH-N
A3Ba, A1A)C5→N1e	N-CH, NH-NH-C
A3Bb, A1A)C5→N1b	NH-NH, C-N-CH
A3Bc, A1A)C5→N1d, A1A)C3→N4c, A4Bd,A2A)N1→N2c	C-NH, NH-CH-N
A4Ba, A1A)C3→N4e	NH-C, NH-N-CH
A2A)N1→N2a	NH-CH, N-NH-C
A4Bc, A1A)C3→N4d, A2A)N1→N2d	N-CH, NH-C-NH
A3A)C5→N4c, A4A)C3→N2c, A3A)C5→N4d, A4A)C3→N2d	NH-C, NH-C-NH

3.4 Determination of activation energy of 1Htri-CH_3 under translation of proton condition

Table 2 shows the bond distances of 1Htri-CH_3 is revealed in table 2 and fig.15 reveals the combinations of two ways of cleavage bounds of thermal decomposition of 1Htri-CH_3 are at (a) N1-C5 and C3-N4 and (c) N1-N2 and C3-N4.

Table 5 shows it can be considered that with these ΔEa values at TS of 1Htri-CH_3. The combination of (c) N1-N2 and C3-N4 shows the lowest ΔEa comparing with (c) cleavage pattern then the decomposition of 1Htri will start preferentially at (c) N1-N2 and C3-N4.

Table 5. Structure of transition state of Htri-CH_3 at the initial step of the thermal decomposition

Cleavage bonds	Distance [Å]					ΔEa [kJ/mol]	$\Delta G_{Tdsc=310°C}$ [kJ/mol]
	N1-N2	N2-C3	C3-N4	N4-C5	C5-N1		
Ba	1.29	1.201	2.178	1.179	2.169	365	382
Bc	2.941	1.180	1.967	1.286	1.281	420	475
A1Ba	1.276	1.179	2.795	1.227	2.034	458	417
A1Bc	2.208	1.208	1.793	1.280	1.230	291	403
A1Bd	Not optimized					Over500	
A2Ba	Not optimized					Over600	
A2Bc	Not optimized					Over500	
A2Bd	Not optimized					Over500	
A1A)N1→N2a	Not optimized					Over500	
A1A)N1→N2c	Not optimized						
A1A)N1→N2d	Not optimized						

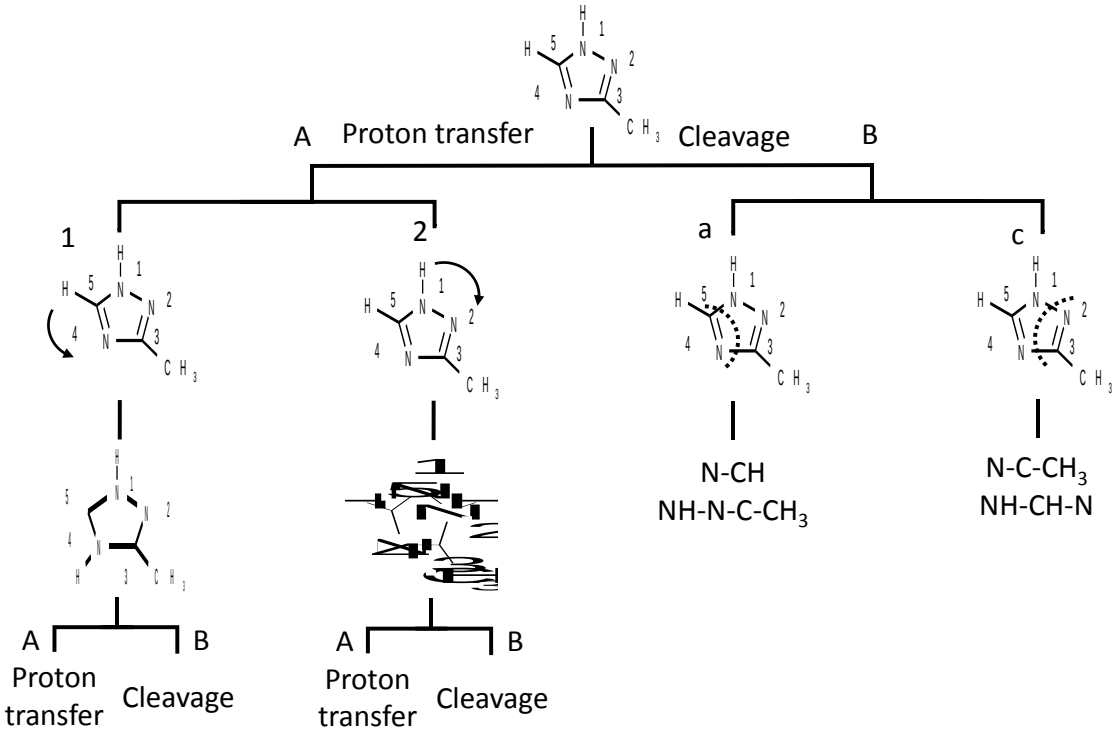

Fig.15 Thermal decomposition pathway map at (A) proton transfer and (B) cleavage of 1Htri-CH_3

Fig.16 shows the next step after proton from (A1) C5→N4 . There are two proton transfer pathways as (A1A) N1→N2 and (A1A)N1→C5 and there are three cleavage bonds as (A1Ba) N1-C5 and C3-N4 (A1Bc) N1-N2 and C3-N4 and (A1Bd) N1-N2 and N4-C5cleavage pathway occur.

Fig.17 shows in case of (A2) proton transfer from N1→N2 at first step of 1Htri-CH_3, we could not observe T.S. of all pathways as (A2A) C5→N4, (A2A) C5→N1,bond cleavage of (A2Ba) N1-C5 and C3-N4, (A2Bc) N1-N2 and C3-N4 and (A2Bd) N1-N2 and N4-C5.

Fig. 18 shows energy flow chart of A1) C5→N4Ba and A1) C5→N4Bc. it can be considered with this energy chart that pathway should be A1) N1→N2c.

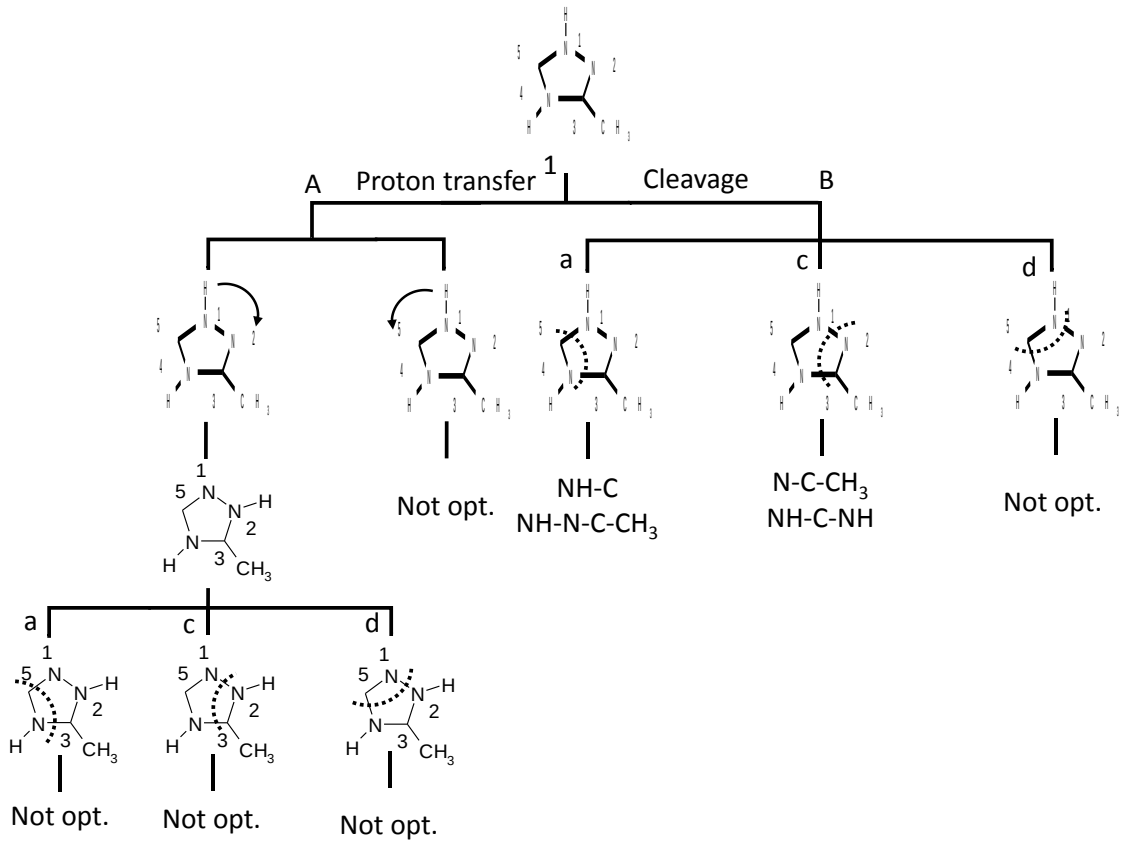

Fig.16 Thermal decomposition pathway (A1A) proton transfer and (A1B) cleavage of 1Htri-CH_3

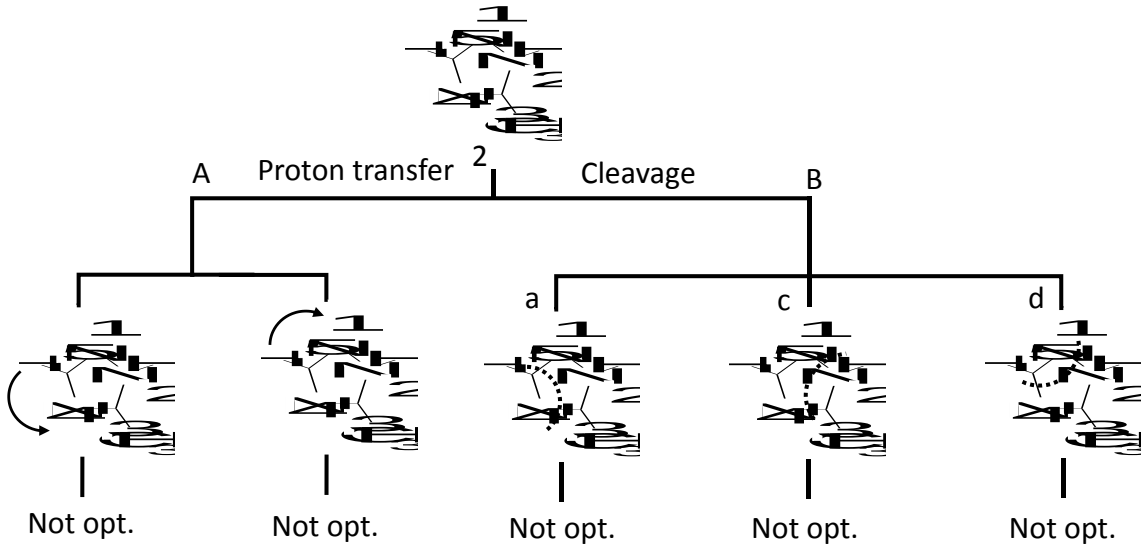

Fig.17 Thermal decomposition pathway (A2A) proton transfer and (A2B) cleavage of 1Htri-CH_3

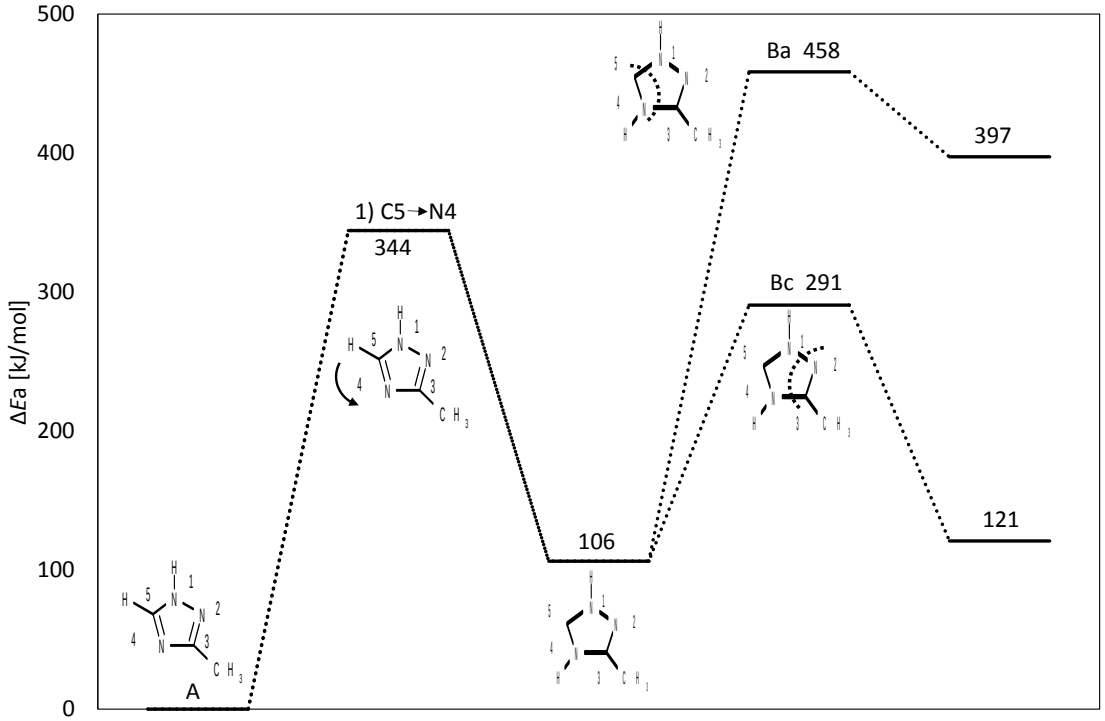

Fig.18 Thermal decomposition pathway at A1)C5→N4Ba, c of 1Htri-CH_3

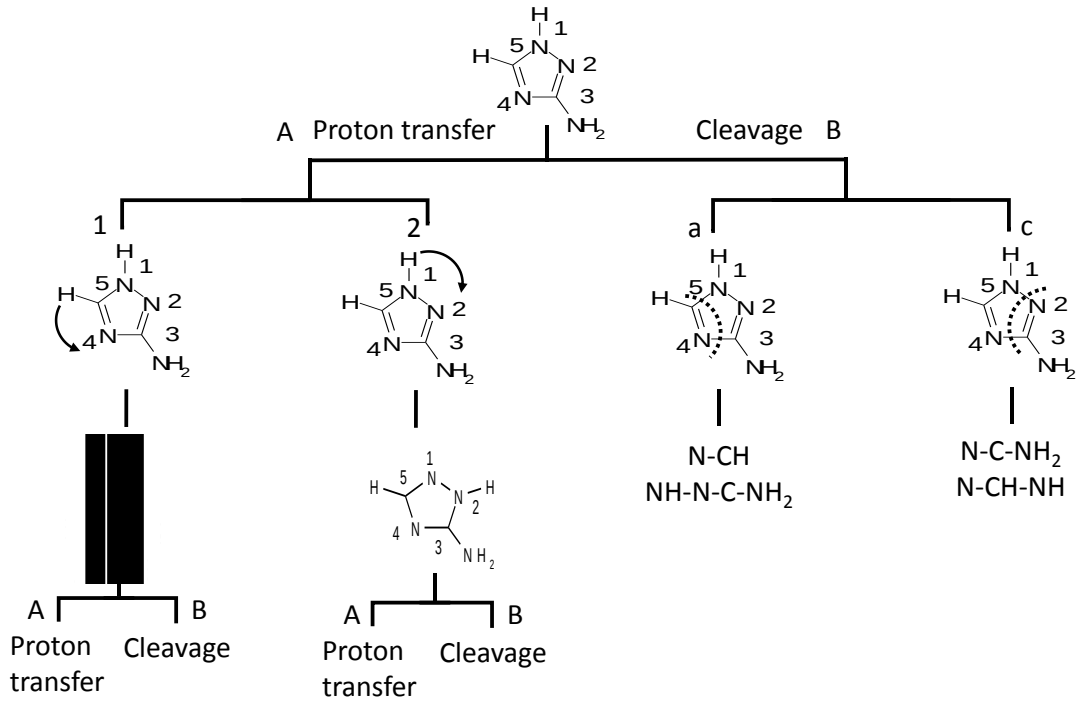

Fig.19 Thermal decomposition pathway at (A) proton transfer and (B) cleavage of 1Htri-NH_2

Table 6. Structure of TS of 1Htri-NH_2

Cleavage bonds	Distance [Å]					ΔEa [kJ/mol]	$\Delta G_{TDSC=296°C}$ [kJ/mol]
	N1-N2	N2-C3	C3-N4	N4-C5	C5-N1		
Ba	1.314	1.189	2.220	1.176	2.221	419	167
Bc	3.080	1.188	1.976	1.281	1.276	434	401
A1Bc	2.205	1.214	1.769	1.282	1.240	290	44
A1A)N1→C5c	2.112	1.172	2.779	1.286	1.270	406	143
A2A)C5→N4c	1.789	1.233	2.880	1.223	1.232	405	253
A2A)C5→N4e	1.290	2.392	1.185	2.485	1.187	478	318
A1Ba	Not optimized					Over500	
A1Bd	Not optimized					Over500	
A2Ba	Not optimized					Over500	
A2Bc	Not optimized					Over500	
A2Bd	Not optimized					Over500	
A1A)N1→C5a	Not optimized					Over500	
A1A)N1→C5d	Not optimized					Over500	
A2A)C5→N4d	Not optimized						

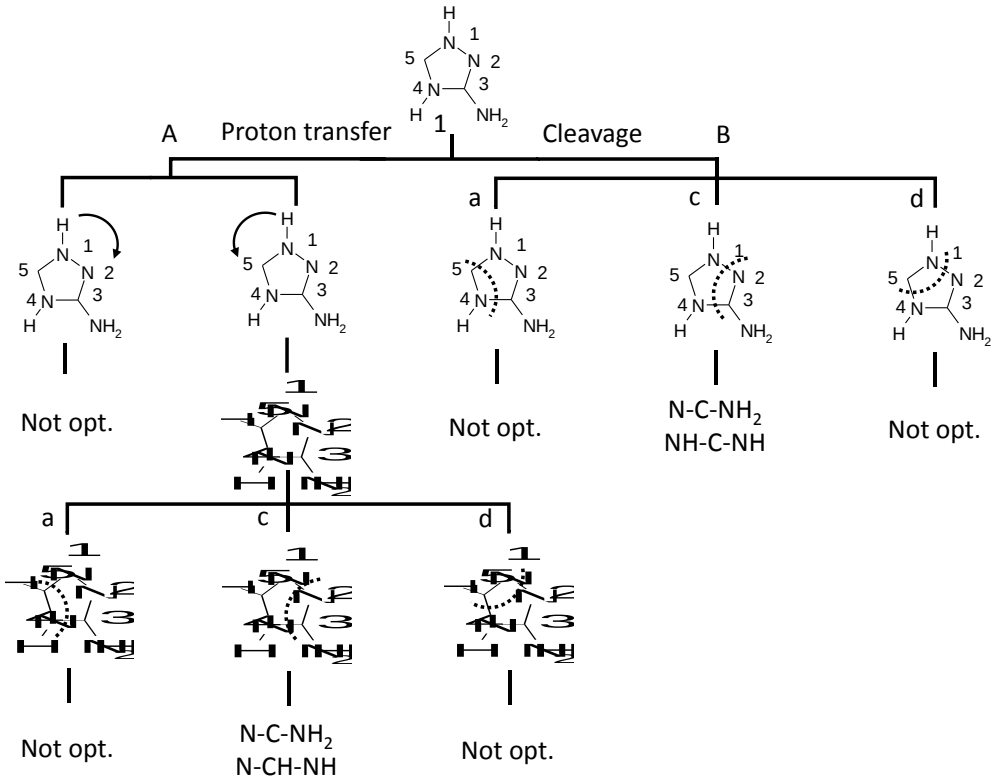

Fig.20 Thermal decomposition pathway (A1A) proton transfer and (A1B) cleavage of 1Htri-NH_2

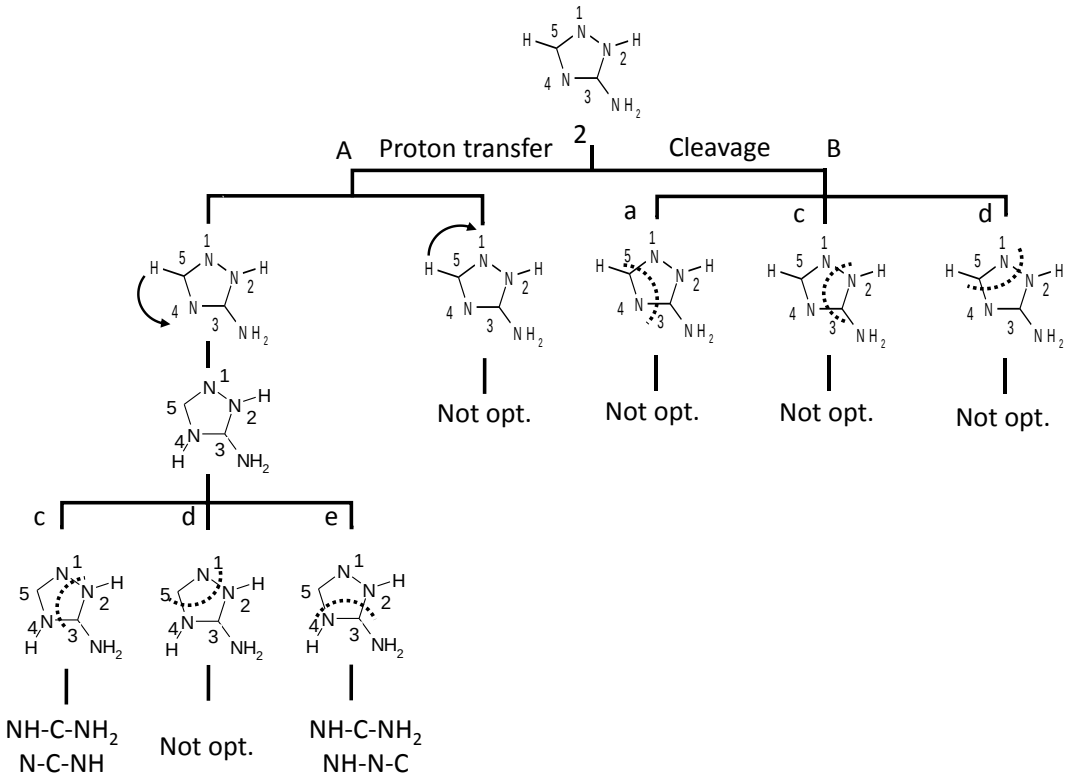

Fig.21 Thermal decomposition pathway (A2A) proton transfer and (A2B) cleavage of 1Htri-NH_2

In fig.19 shows there are also two possible thermal decomposition pathways assumption of 1Htri-NH_2 as (A) proton transfer at first state and (B) bond cleavage at first state. As same as in the case of 1Htri and 1Htri-NH_2.

Table 2 shows the bond distances of 1Htri-NH_2 is revealed in table 2 and fig.19 reveals the combinations of two ways of cleavage bounds of thermal decomposition of 1Htri-NH_2 are at (Ba) N1-C5 and C3-N4 and (Bc) N1-N2 and C3-N4 are shown in table 6.

Fig.20 shows the next step after proton from (A1) C5→N4 . There are two proton transfer pathways as (A1A) N1→N2 and (A1A)N1→C5 and there are three cleavage bonds as (A1Ba) N1-C5 and C3-N4 (A1Bc) N1-N2 and C3-N4 and (A1Bd) N1-N2 and N4-C5cleavage pathway occur.

Fig.21 shows in case of (A2) proton transfer from N1→N2 at first step of 1Htri-CH3, we could not observe T.S. of all pathways as (A2A) C5→N1,bond cleavage of (A2Ba) N1-C5 and C3-N4, (A2Bc) N1-N2 and C3-N4 and (A2Bd) N1-N2 and N4-C5.

Fig. 22 shows energy flow chart of A1) N1→C5c and A1Bc and fig.23 A2A C5→N4Bc and e. it can be considered with this energy chart of 1Htri-NH2 that pathway should be A1) N1→C4c.

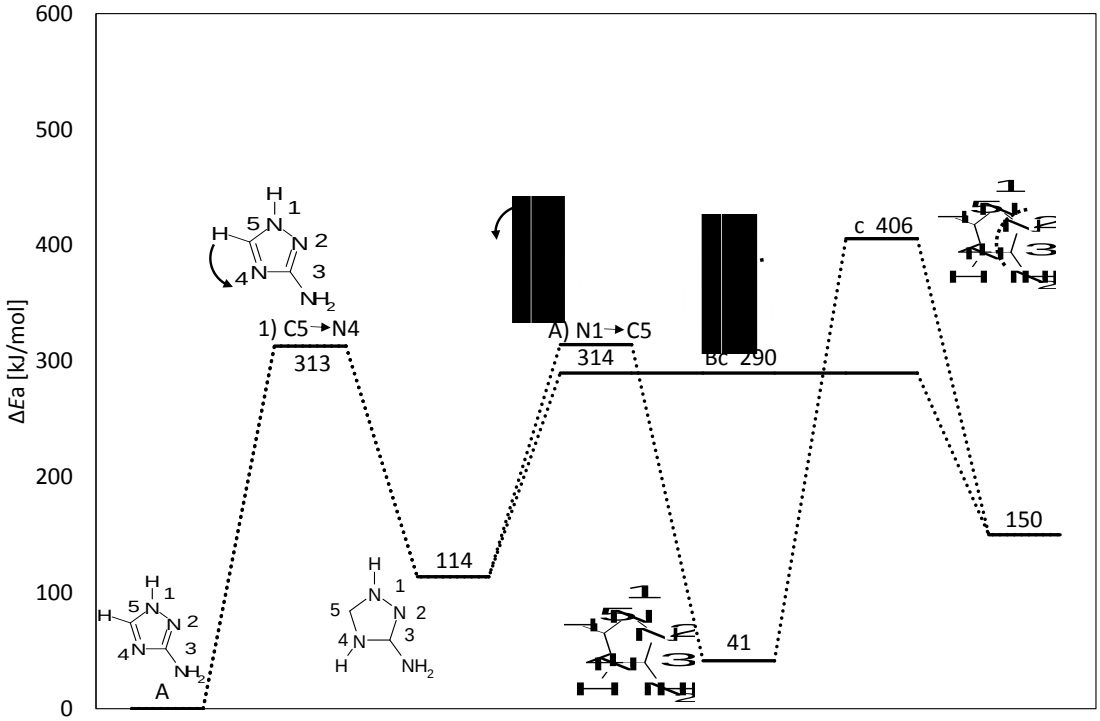

Fig.22 Thermal decomposition pathway map at A2 of 1Htri-NH_2

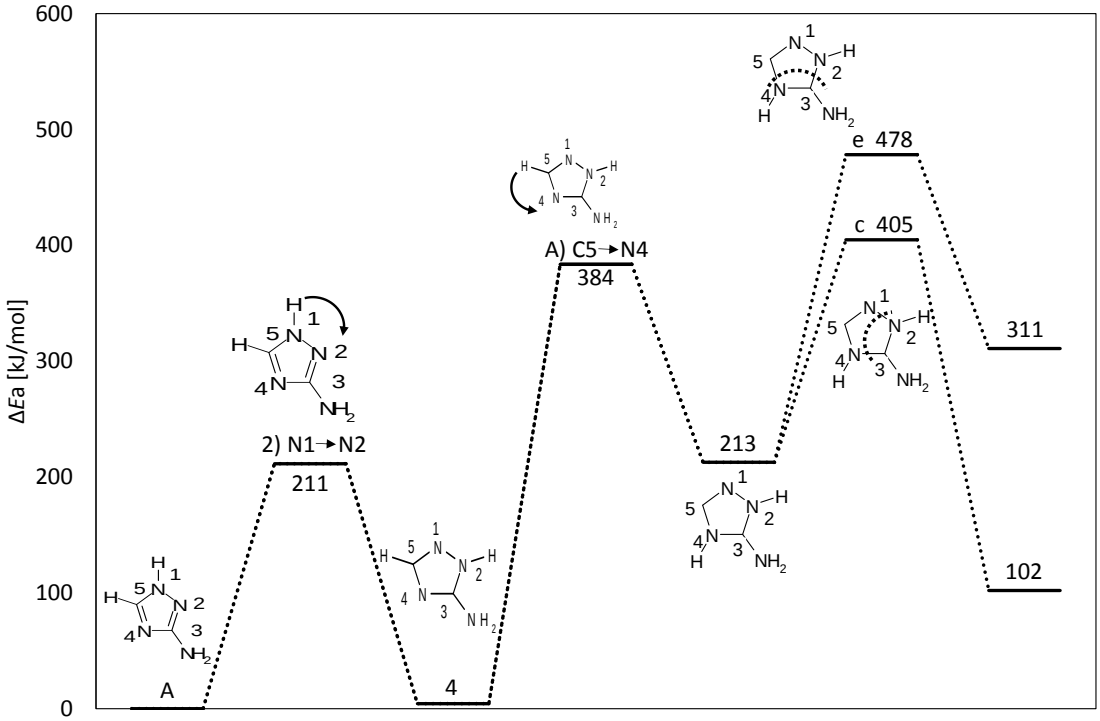

Fig.23 Thermal decomposition pathway map at A2 of 1Htri-NH_2

Table 7 The produced gases after each decomposition pathway of 1Htri-CH_3

Cleavage bonds	Gas
Ba	N-CH, NH-N-C-CH_3
Bc	N-C-CH_3, NH-CH-N
A1Ba	NH-C, NH-N-C-CH_3
A1Bc	N-C-CH_3, NH-C-NH

Table 8. The produced gases after each decomposition pathway of 1Htri-NH_2

Cleavage bonds	Gas
Ba	N-CH, NH-N-C-NH_2
Bc	N-C-NH_2, N-CH-NH
A1Bc	N-C-NH_2, NH-C-NH
A1A)N1→C5c	N-C-NH_2, N-CH-NH
A2A)C5→N4c	NH-C-NH_2, N-C-NH
A2A)C5→N4e	NH-C-NH_2, NH-N-C

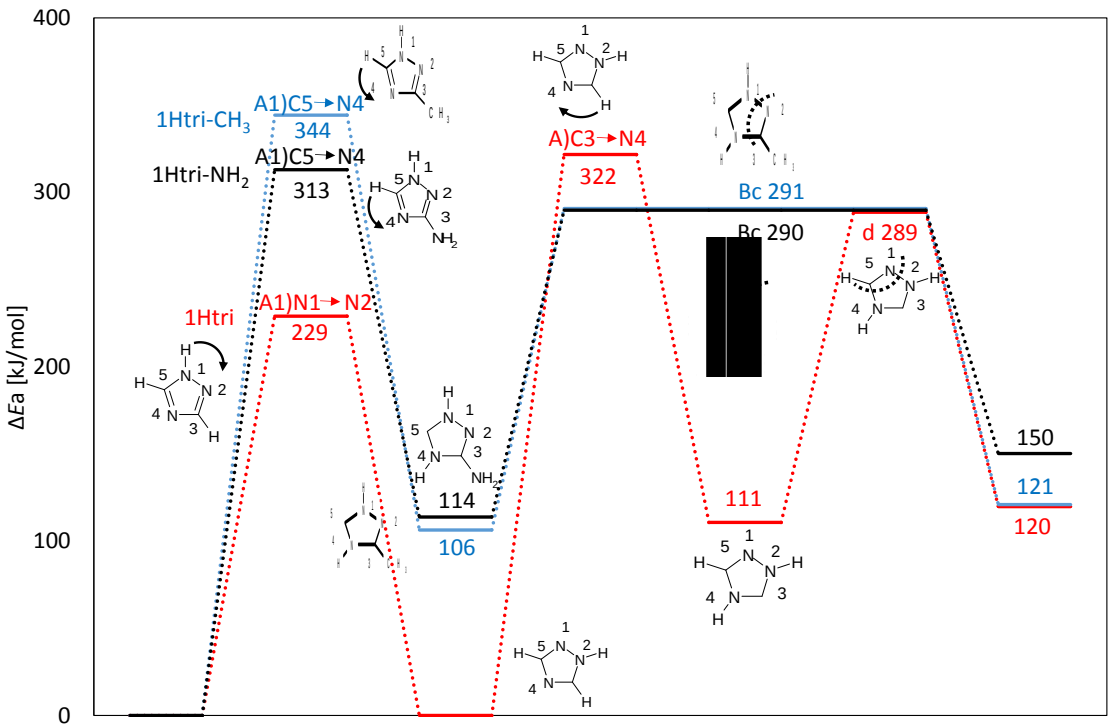

Fig.24 Summary of the selected thermal decomposition pathways of 1Htri, 1Htri-CH_3 and 1Htri-NH_2

3.5 Thermal decomposition of 1Htri, 1Htri-CH_3 and 1Htri-NH_2

As result from section 3.3 the appropriate thermal decomposition pathway of 1Htri, 1Htri-CH_3 and 1Htri-NH_2 were outcome by lower ⊿*E*a selection. Then using *G=H-TS* equation, the original structure of each 1Htri, 1Htri-CH_3 and 1Htri-NH_2 and its final product from selected pathway from section 3.3 were calculated during 25- 300 ºC as show in fig.24 – 28. Then at cross section point, the predicted T_{DSC} was received. In this study, fig. 26 shows the determined T_{DSC} was 297 ºC of 1Htri, fig.27 shows T_{DSC} was 114 ºC of 1Hti-CH_3 and fig.28 shows T_{DSC} was 289 ºC of 1Htri-NH_2.

Fig. 29 summarize the measured and calculated T_{DSC}. Almost the calculated T_{DSC} were match with the measured T_{DSC}.

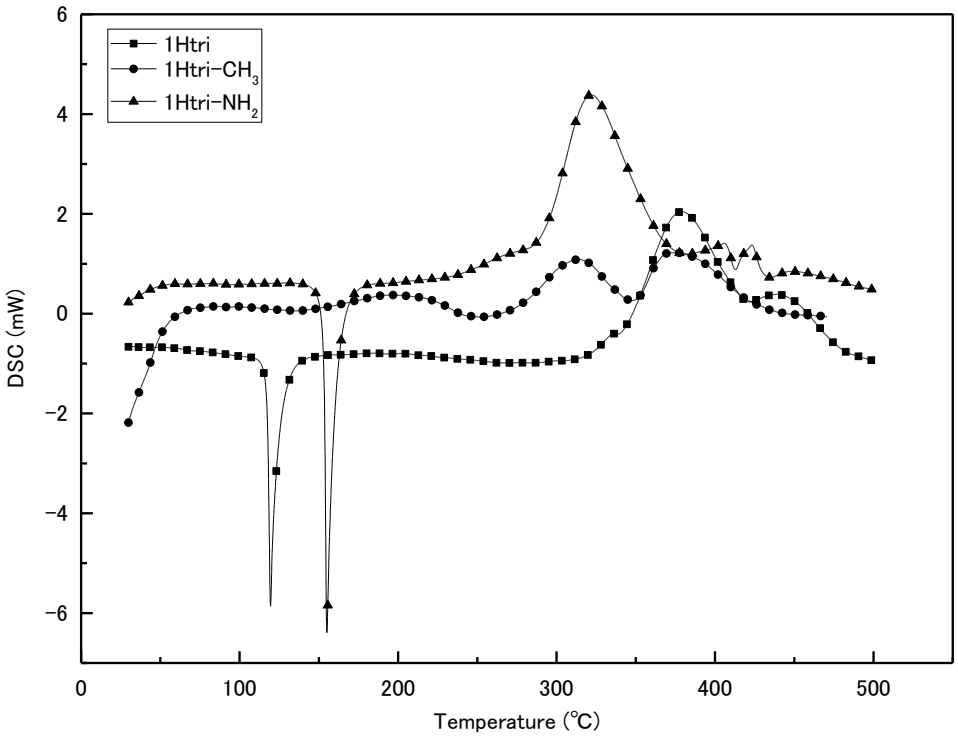

Fig.25 DSC curves of 1Htri, 1Htri-CH_3 and 1Htri-NH_2

Table 9 summary of the calculated T_{DSC} of 1Htri, 1Htri-CH_3 and 1Htri-NH_2 comparing with the measured T_{DSC}

	$T_{DSC(measured)}$ [°C]		$\Delta G_{25°C}$ [kJ/mol]	$\Delta G_{T_{DSC}}$ [kJ/mol]	$T_{DSC(calc.)}$ [°C]
1Htri	338	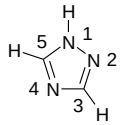	0	94	297
		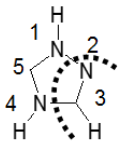	-49	101	
1Htri-NH_2	293	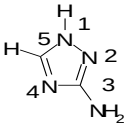	0	91	289
		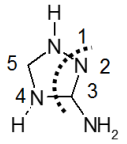	-50	92	
1Htri-CH_3	172	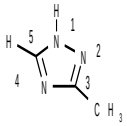	0	46	114
		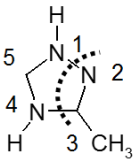	-18	57	

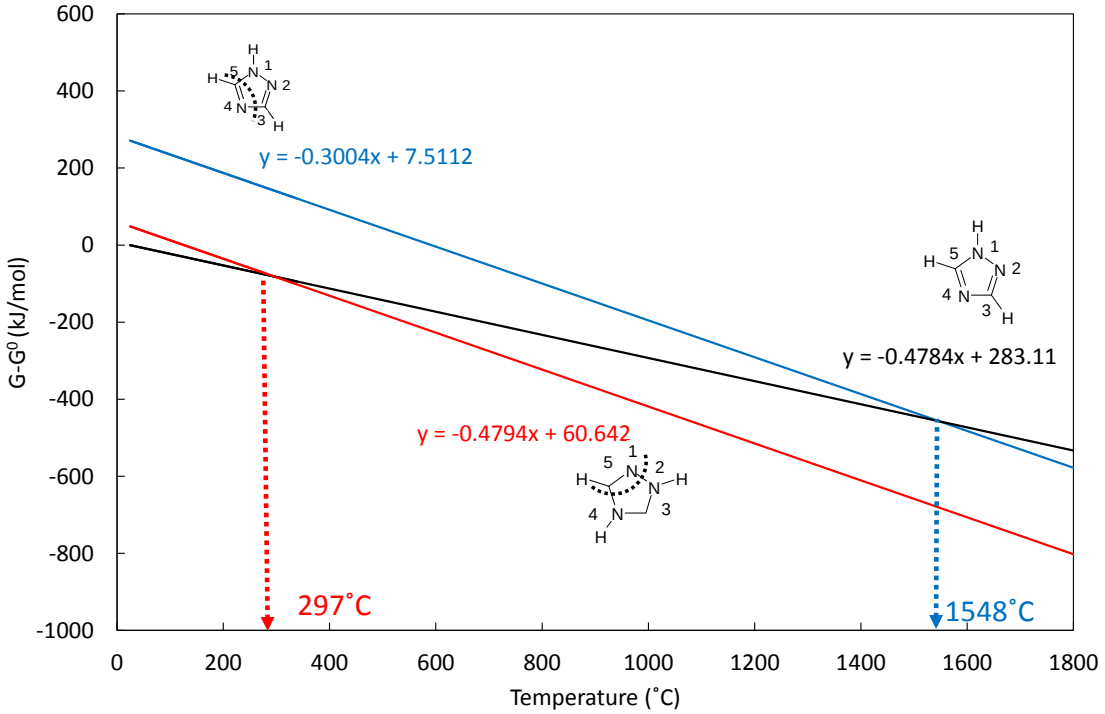

Fig.26 Calculated T_{DSC} of 1Htri from proton pathway (red color) and cleavage pathway (blue color)

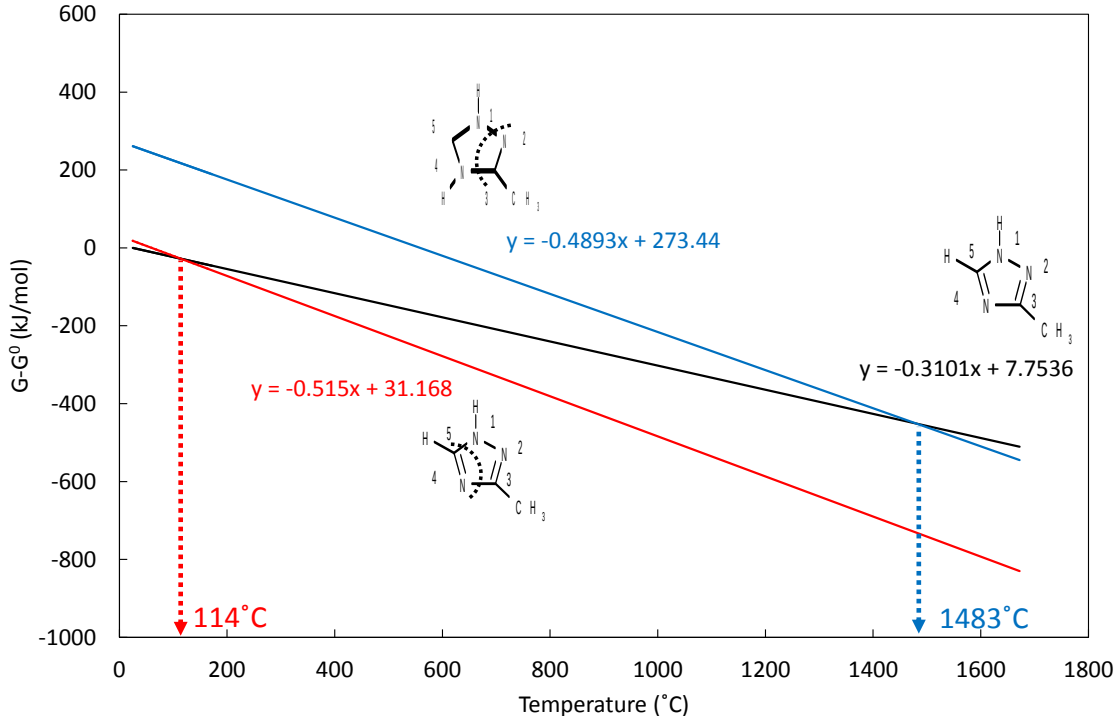

Fig.27 Calculated T_{DSC} of 1Htri-CH_3 from proton pathway (red color) and cleavage pathway (blue color)

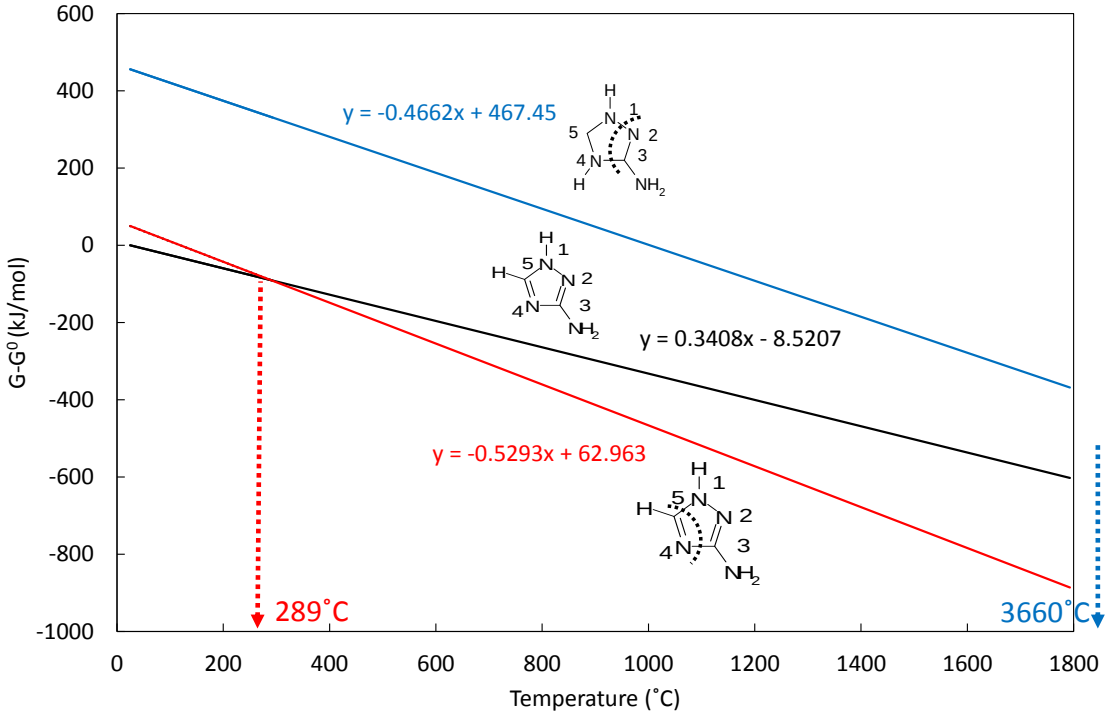

Fig.28 Calculated T_{DSC} of 1Htri-NH_2 from proton pathway (red color) and cleavage pathway (blue color)

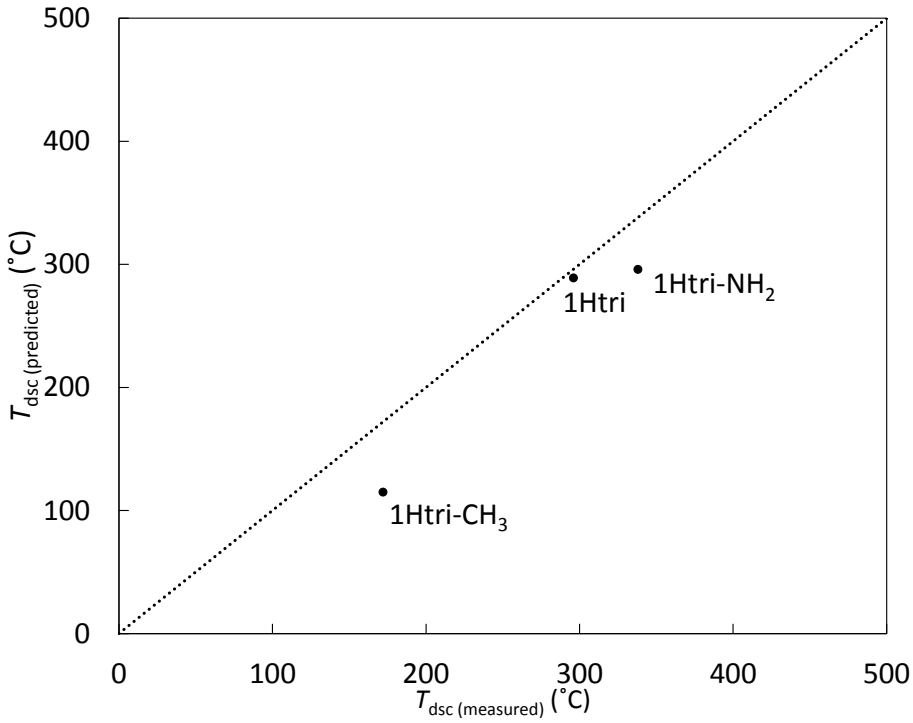

Fig.29 comparing the calculated T_{DSC} from this study with the measured T_{DSC} by DSC

4. Conclusion

In the present work, T_{DSC} of 1Htri, 1Htri-CH_3 and 1Htri-NH_2 were determined by using SC-DSC and MO was used to clarify thermal decomposition mechanism and stability criteria of pathway of 1Htri, 1Htri-CH_3 and 1Htri-NH_2 were calculated.

T_{DSC} of each compound was determined from the lower ΔEa of thermal decomposition pathway model as proton transfer combine with cleavage bond. The determined T_{DSC} was compared with the measured T_{DSC}.

The results shows that the determined T_{DSC} from of decomposition pathway model 1Htri, 1Htri-CH_3 and 1Htri-NH_2 corresponding with the measured T_{DSC}.

References

1. S. Tagomori, Y. Kuwahara, H. Masamoto, M. Shigematsu, W. Kowhakul. Influence of substituent to the thermal decomposition of 1H-1,2,4-triazole. 4th International Conference on Biology, Environment and Chemistry (ICBEC), 66-70, 2013.
2. H. Kiuchi, W. Kowhakul, M. Arai, M. Tamura, Y. Wada, M. Kumasaki. A study on thermal behavior of triazoles. 62nd Japan Explosives Society Conference. Tokyo: 2003, pp.35-38.
3. W. Kowhakul, M. Kumasaki, M. Arai. Study on thermal behavior of 1H-1,2,4 triazole-copper complex with substituents. Science and Technology of Energetic Materials. 2005, 66 (6): 425-430.
4. W. Kowhakul, R. Miyazaki, M. Kumasaki, Y. Wada, M. Arai, M, Tamura. A study on the characteristics of azole-metal complexes. Kayaku Gakkaishi. 2002, 63 (6): 362-366.
5. T. Masoumeh, S. Mahboubeh A., G. Mitra, S. Mahmoud. 1,3-Sigmatropic hydrogen shift in 3-amino-1H-1,2,4-triazole during the complexation of this ligand with cobalt (II) ion, single crystal structure of a new trinuclear Co(II) 1,2,4-triazole complex. Journal of Chemical Crystallography. 2011, 41 (2): 127-131.
6. M. Tamura, M. Arai, and Y. Akutsu. Energy material and safety. Asakura Publishing, 1999, pp.
7. K.S.Rao and A.K.Chaudhary , Investigation of the thermal decomposition and stability of energetic 1,2,4-triazole derivatives using a UV laser based pulsed photoacoustic technique RSC Adv., 2016,6,47646-47654
8. M M.Tabatabee et.al., 1,3-sigmatropic Hydrogen Shift in 3-Amino-1H-1,2,4-Triazole During the Complexation of this Ligand with Cobalt(Ⅱ) Ion, Single Crystal Structure of a New Trinuclear Co(Ⅱ) 1,2,4-Triazole Complex, J Chem Crystallogr (2011) 41:127-131